UNIVERSITI TEKNOLOGI MARA

MATHEMATICS LETTERS
https://sites.google.com/tmsk.uitm.edu.my/mathematicsletters

Breast Tissue Classification Using Modified Otsu Thresholding and Disk Structuring Elements

[1, *]Siti Salmah Yasiran, [2] Abdul Muhaymin Abdullah, [3] Muhammad Hasif Abd Razak, [4] Suhaila Abd Halim & [5] Nor Farihah Azman
[1,2,3,4,5]Centre of Mathematical Sciences, Faculty of Computer and Mathematical Sciences, Universiti Teknologi MARA, 40450 Shah Alam, Selangor. Malaysia.
[*1]salmahyasiran@uitm.edu.my
[2] 2020827778@student.uitm.edu.my,
[3] 22020834562@student.uitm.edu.my
[4]suhaila889@uitm.edu.my
[5]farihahazman@uitm.edu.my
*Corresponding author

Received: 5/10/2026 Revised: 20/10/2026 Accepted: 25/10/2026 Published: 31/10/2026

ABSTRACT

Breast tissue density is an important factor in mammographic interpretation, and a computer-aided diagnosis (CAD) pipeline can support the classification of fatty, glandular and dense tissue. This study compares two segmentation pipelines: hybrid original Otsu thresholding with mathematical morphology and hybrid modified Otsu thresholding with mathematical morphology. Ninety-five mammographic images from the Mammographic Image Analysis Society (MIAS) database were used. The images were preprocessed using median filtering and histogram stretching, segmented using the two Otsu-based methods, and refined by erosion with disk-shaped structuring elements having radii from 20 to 200 pixels. Binary Robust Invariant Scalable Keypoints (BRISK) were used for feature extraction and detection, while Principal Component Analysis (PCA) with 95% explained variance was evaluated for feature reduction. Support Vector Machine (SVM) classifiers with Gaussian, linear, quadratic, and cubic kernels were then compared using a 70% training and 30% testing split. On the testing data, the hybrid original Otsu pipeline at radius 200 achieved 88.9% accuracy without PCA and 87.1% with PCA, whereas the hybrid modified Otsu pipeline at radius 80 achieved 87.1% without PCA and 85.2% with PCA. The original Otsu hybrid therefore produced the highest reported testing accuracy, while the results also demonstrate that the disk radius affects classification performance and should be selected empirically for the image set.

Keywords: breast tissue classification, mathematical morphology, Otsu thresholding, support vector machine, structuring element.

INTRODUCTION

Breast cancer is one of the major health concerns affecting women worldwide, and early detection is

important for improving the effectiveness of treatment. Mammography is widely used for breast cancer screening and diagnosis because it can detect abnormalities before obvious symptoms appear. However, the interpretation of mammographic images remains challenging and depends heavily on the expertise of radiologists. Consequently, image-processing techniques have been widely explored to support computer-aided diagnosis systems in improving the analysis of breast images (Dallali et al., 2018). Breast tissue can generally be classified into fatty, glandular, and dense tissue, and these tissue characteristics are closely related to breast density. High breast density may increase breast cancer risk and may also reduce the sensitivity of mammography (Nishiyama et al., 2020). Image segmentation is an important stage in medical image analysis (Azman et al., 2024) because it separates an image into meaningful regions before further processes such as feature extraction and classification. Various segmentation techniques have been developed, including region-based methods, edge-based methods, and thresholding approaches. Thresholding transforms a grayscale image into foreground and background regions based on selected intensity values. Global thresholding methods are generally simple and computationally efficient, making them suitable for many grayscale image-processing applications (Khairnar et al., 2021).

One of the most widely used global thresholding techniques is the Otsu method. Otsu thresholding determines an optimal threshold by separating pixels into foreground and background classes based on class variance. However, its performance may be affected by image noise, target size, and differences in intra-class variance, which can reduce segmentation accuracy under certain image conditions (Kumar & Tiwari, 2019; Chunlei et al., 2019). To improve the segmentation result, Otsu thresholding can be combined with mathematical morphology. Mathematical morphology provides operations such as erosion and dilation that can refine object boundaries and preserve important geometric structures in the segmented image (Liu et al., 2021). The standard Otsu formulation may also be modified by replacing the mean-based term with a standard-deviation-based formulation. Yasiran et al. (2020) applied a modified Otsu approach based on standard deviation and subsequently combined it with mathematical morphology for breast cancer classification. The use of mathematical morphology after thresholding can improve the shape representation of the segmented region while removing unnecessary image components.

An important component of mathematical morphology is the structuring element, which determines how the morphological operation interacts with the image (Noor et al., 2025). Gudinas et al. (2020) demonstrated that MATLAB structuring elements can be generated with user-defined radii and that changing the radius alters the resulting morphological operation. Disk-shaped structuring elements are particularly useful because their symmetric shape allows them to capture circular neighbourhoods around image pixels, while different radius values can control the extent of erosion or dilation applied to the image. Following segmentation, suitable features must be extracted before classification. Binary Robust Invariant Scalable Keypoints (BRISK) has been used for feature extraction and detection because of its relatively simple computation and its ability to provide scale and rotation invariance (Mohamad et al., 2018). Dimensionality reduction may then be applied to reduce the number of input features. Principal Component Analysis (PCA) is commonly used to transform correlated variables into a smaller set of uncorrelated components while retaining important information from the original feature space (Remeseiro & Bolon-Canedo, 2019).

For classification, Support Vector Machine (SVM) is a supervised learning method that can be applied to classification and regression problems. SVM separates classes by constructing a decision hyperplane, and different kernel functions, including linear, quadratic, cubic, and Gaussian kernels, can be employed to model the data. Singh and Kumar (2020) reported that the cubic SVM classifier performed well in breast histopathological image classification. Although previous studies have investigated Otsu

thresholding, modified Otsu formulations, mathematical morphology, feature extraction, and SVM classification, the effect of varying the radius of a disk-shaped structuring element within this classification framework has received less attention. Disk structuring elements were not systematically evaluated using multiple radius values during the classification process. Therefore, this study compares hybrid original Otsu with mathematical morphology and hybrid modified Otsu with mathematical morphology using different disk structuring-element radii for the classification of fatty, glandular, and dense breast tissue. The performance of both approaches is evaluated in terms of classification accuracy and computational efficiency.

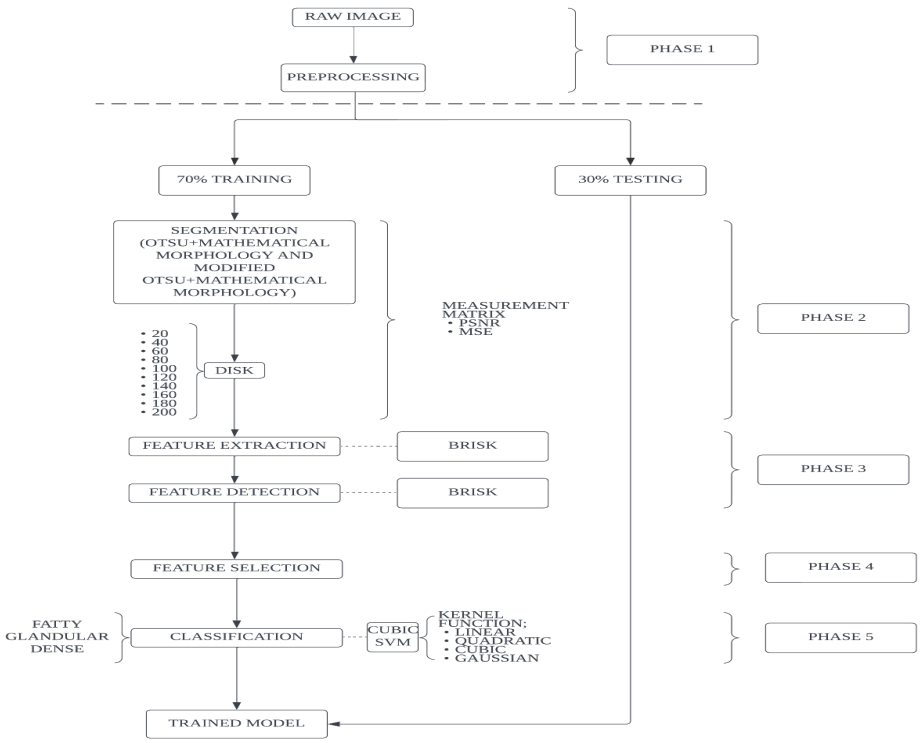
THE PROPOSED METHOD

Proposed Framework

The proposed framework consists of five main phases: preprocessing, segmentation, feature extraction and detection, feature selection, and classification, as illustrated in Figure 1. The study used 95 mammographic images obtained from the Mammographic Image Analysis Society (MIAS) database. The dataset comprised three breast tissue classes: fatty, glandular, and dense. For fatty tissue, 23 images were allocated to the 70% training subset and 13 images to the 30% testing subset. For glandular tissue, 20 and 9 images were used for training and testing, respectively, while 21 and 9 dense-tissue images were assigned to the corresponding subsets. The complete dataset was therefore divided into 70% training data and 30% testing data. MATLAB R2019a was used for image processing, feature analysis, and classification throughout the experimental procedure.

Figure 1

Flowchart of the Proposed Study



Phase 1: Preprocessing

Preprocessing was performed to improve the quality of the mammographic images before segmentation by reducing unwanted background information and enhancing the visibility of breast tissue. A median filter was first applied to reduce image noise while preserving important edge information under suitable conditions (Palani et al., 2020). Histogram stretching was subsequently employed to enhance image contrast. This technique was selected because it improves the distribution of grey-level intensities without introducing excessive local enhancement. The resulting preprocessed images were then used as the input for the segmentation phase.

Phase 2: Segmentation

Otsu and Modified Otsu Thresholding

Two thresholding approaches were investigated in this study: the original Otsu method and the modified Otsu method. The original Otsu method determines an optimal threshold by examining the distribution of pixel intensities between the foreground and background classes. The method evaluates the possible threshold values and identifies the threshold that provides the most effective separation between the two classes. The within-class variance used in the original Otsu formulation is expressed in Equation 1:

$$\sigma_{\omega}^{2}(Q) = \sum_{j=0}^{Q=1} \rho(j).\sigma_{\beta}^{2} + \sum_{j=0}^{N-1} \rho(j) + \sigma_{\omega}^{2}\,(Q) \tag{1}$$

The corresponding between-class variance is obtained from the total and within-class variance, as stated in Equation 2, while Equation 3 expresses the between-class variance in terms of the background and foreground class means.

$$\sigma_{\psi}^{2}(Q) = \sigma^{2}(Q) - \sigma_{\varsigma}^{2}(Q) \tag{2}$$

$$\sigma_{\psi}^{2}(Q) = \sum_{j=0}^{Q=1} \rho(j).[m_{\beta}(Q) - m]^{2} + \sum_{j=0}^{N-1} \rho(j).[m_{\omega}(Q) - m]^{2} \tag{3}$$

The modified Otsu formulation replaces the mean-based quantity used in the original formulation with a standard-deviation-based term. The standard deviation is defined in Equation 4, and the modified between-class expression is given in Equation 5.

$$SD = \sqrt{\frac{\sum_{j=0}^{N}(k_j - \check{\mathrm{K}})^{2}}{N}} \tag{4}$$

$$\sigma_{\psi}^{2}(Q) = \sum_{j=0}^{Q=1} \rho(j).\sum_{j=0}^{N-1} \rho(j).[SD_{\beta} - SD_{\omega}]^{2} \tag{5}$$

The threshold selected from this formulation was then used before mathematical morphology.

Mathematical Morphology and Disk Structuring Element

Mathematical morphology (MM) was applied after thresholding to refine the segmented image. Although erosion and dilation represent the two fundamental morphological operations, the segmentation procedure in this study specifically employed the erosion operator. Let A denote the image set, and B denote the corresponding structuring element (SE). The erosion and dilation operations are defined in Equations 6 and 7, respectively.

$$A \ominus B = \{G|(B)_z \subseteq A\}, A, B \in G^2 \quad (6)$$

$$A \oplus B = \{G|(B)_z \cap A \neq \emptyset\}, A, B \in G^2 \quad (7)$$

A disk-shaped structuring element was generated in MATLAB using the strel function. Ten radii were investigated: 20, 40, 60, 80, 100, 120, 140, 160, 180, and 200 pixels. The segmented binary image was eroded using the selected disk structuring element (SE) as shown in Figure 2, and the boundary was obtained using MATLAB's "bwperim" operation.

Figure 2

Disk-shaped Structuring Element



Phase 3: Feature Extraction and Feature Detection

BRISK was applied for both feature extraction and feature detection from the segmented images. BRISK provides a binary descriptor constructed from intensity comparisons and is designed to support scale and rotation invariance (Leutenegger et al., 2011).

Phase 4: Feature Selection

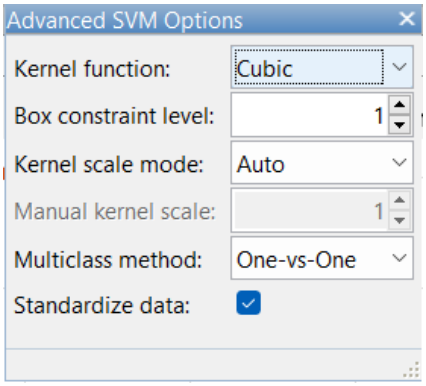
After feature extraction, PCA was evaluated as an optional feature-reduction stage. The PCA setting retained 95% explained variance, and the number of numeric components was set to one in the MATLAB Classification Learner configuration.

Phase 5: Classification

Classification was performed using SVM in MATLAB's Classification Learner application. Four kernel functions were investigated: Gaussian, linear, quadratic, and cubic. The box constraint was set to 1, the kernel scale was set to automatic, one-versus-one classification was used for the multiclass problem, and the data were standardized as shown in Figure 3. Each kernel was evaluated for each disk radius from 20 to 200 pixels, both with and without PCA. The study recorded classification accuracy, prediction speed in observations per second, and training time in seconds.

Figure 3

SVM Settings in MATLAB Classification Learner



ANALYSIS AND RESULTS

In this section, the classification results of 3 types of breast tissue using two distinct approaches, that is, with PCA and without PCA, are recorded and analyzed. This is to determine which approach yielded the best kernel and to evaluate both approaches' accuracy. For this study, 70% of the data will be utilized for training, while the remaining 30% will be used for testing. The accuracy performance of the training dataset is displayed in Table 1 and Table 2, respectively, and compares hybrid original Otsu with mathematical morphology with hybrid modified Otsu with mathematical morphology.

Analysis 1: Performance of Hybrid Original Otsu with Mathematical Morphology

Table 1

Accuracy Performance of Hybrid Original Otsu with Mathematical Morphology

Radius	Kernel Function	Without PCA			With PCA		
		%	Prediction Speed (obs/sec)	Training Time (sec)	%	Prediction Speed (obs/sec)	Training Time (sec)
20	Gaussian	68.1	~190260	346.82	72.4	~200	301.85
	Linear	44.5	~50000	63.484	44.5	~29000	200.16
	Quadratic	54.7	~210	510.79	52.6	~500	368.14
	Cubic	82.6	~220	465.94	83.0	~580	334.11
40	Gaussian	67.6	~220	360.5	69.1	~270	304.41
	Linear	44.4	~11000	238.65	44.4	~25000	181.08
	Quadratic	54.3	~249	487.45	52.7	~460	282.29
	Cubic	81.4	~290	558.39	81.1	~460	292.64
60	Gaussian	69.9	~200	1194.8	69.4	~290	650.01
	Linear	44.7	~5500	419.23	44.7	~16000	170.86
	Quadratic	54.3	~270	638.35	52.5	~290	340.43
	Cubic	82.0	~240	461.97	82.1	~310	427.43
80	Gaussian	70.8	~260	300.51	69.2	~210	343.43
	Linear	44.7	~21000	201.55	44.7	~36000	83.312
	Quadratic	54.7	~220	499.91	52.6	~310	397.05
	Cubic	83.3	~180	582.07	83.0	~320	366.56
100	Gaussian	69.9	~230	650.67	70.9	~200	413.31
	Linear	44.7	~27000	260.05	44.7	~16000	370.43
	Quadratic	54.0	~240	509.38	52.8	~450	511.33
	Cubic	82.3	~280	548.52	84.2	~580	594.41
120	Gaussian	70.7	~210	534.38	70.8	~280	314.08

	Linear	44.7	~33000	211.14	44.7	~89000	44.507
	Quadratic	54.3	~140	579.72	52.6	~440	274.82
	Cubic	83.4	~190	607.53	83.4	~520	311.6
140	Gaussian	69.0	~240	306.31	70.3	~330	243.81
	Linear	44.7	~36000	250.28	44.7	~28000	94.595
	Quadratic	54.4	~340	435.33	52.6	~390	334.58
	Cubic	81.4	~230	449.36	83.1	~440	353.4
160	Gaussian	70.5	~170	1257.5	69.4	~210	1111.2
	Linear	44.7	~23000	619.12	44.7	~25000	1066.3
	Quadratic	54.2	~330	662.65	52.6	~340	970.73
	Cubic	83.6	~290	638.39	82.9	~580	910.93
180	Gaussian	70.1	~230	385.74	71.1	~230	366.85
	Linear	44.7	~61000	119.13	44.7	~47000	71.3
	Quadratic	54.6	~260	445.58	52.7	~290	417.89
	Cubic	83.4	~210	452.65	82.9	~290	384.77
200	Gaussian	69.3	~190	515.37	68.5	~310	307.26
	Linear	44.7	~11000	209.58	44.7	~71000	86.429
	Quadratic	55.4	~200	485.47	52.6	~350	311.3
	Cubic	80.0	~280	460.02	**84.4**	~330	310.08

Table 1 presents the classification performance of the hybrid original Otsu with mathematical morphology for all ten disk radii and four SVM kernel functions. The results are reported separately for experiments conducted with and without PCA. In addition to classification accuracy (%), prediction speed (observation/seconds), and training time (seconds) were recorded to provide information on the computational performance of the different configurations. Without PCA, the cubic kernel consistently produced considerably higher classification accuracy than the gaussian, linear, and quadratic kernels. Across the investigated radii, the cubic-kernel accuracy ranged from 80.0% to 83.6%, with the highest recorded accuracy of 83.6% at radius 160. When PCA was applied, the cubic kernel similarly produced the highest classification accuracies, reaching 84.4% at radius 200. At the same radius, the corresponding accuracy without PCA was 80.0%. Therefore, the results demonstrate that classification performance was affected by both the SVM kernel and the radius of the disk structuring element. Increasing the radius did not produce a monotonic improvement in accuracy. Instead, the performance varied according to the interaction between radius, kernel function, and the use of PCA. Among the four kernels investigated, the cubic kernel produced the strongest classification performance for the hybrid original Otsu approach.

Analysis 2: Performance of Hybrid Modified Otsu with Mathematical Morphology

Table 2

Accuracy Performance of Hybrid Modified Otsu with Mathematical Morphology

Radius	**Kernel Function**	**Without PCA**			**With PCA**		
		%	Prediction Speed (obs/sec)	Training Time (sec)	%	Prediction Speed (obs/sec)	Training Time (sec)
20	Gaussian	71.1	~400	136.41	68.7	~750	117.87
	Linear	44.5	~76000	36.202	44.5	~39000	45.609
	Cubic	80.6	~860	177.04	81.5	~1200	194.6
	Quadratic	54.6	~710	184.7	52.6	~1300	180.99
40	Gaussian	69.6	~370	163.83	70.6	~530	146.83
	Linear	44.4	~67000	34.992	44.4	~46000	46.893

	Cubic	82.2	~650	265.81	82.5	~1400	235.31
	Quadratic	54.6	~680	217.86	52.8	~940	225.49
60	Gaussian	69.8	~460	137.82	69.8	~540	124.41
	Linear	44.7	~50000	34.573	44.7	~61000	32.536
	Cubic	82.6	~890	240.76	81.9	~2100	202.02
	Quadratic	54.7	~610	201.45	52.6	~2700	101.24
80	Gaussian	67.5	~520	123.94	70.7	~1600	48.727
	Linear	44.7	~130000	31.195	44.7	~66000	33.369
	Cubic	**84.5**	~1300	232.77	82.5	~1200	196.42
	Quadratic	54.7	~940	173.19	52.6	~1300	~163.95
100	Gaussian	70.3	~380	144.54	70.0	~540	133.26
	Linear	44.7	~130000	32.79	44.7	~60000	33.537
	Cubic	81.7	~800	240.74	80.5	~850	211.96
	Quadratic	54.7	~560	205.4	52.5	~870	204.01
120	Gaussian	68.3	~380	145.98	69.1	~560	124.33
	Linear	44.7	~130000	31.657	44.7	~51000	36.822
	Cubic	82.2	~840	245.27	83.0	~920	217.51
	Quadratic	54.7	~790	198.2	52.6	~860	202.91
140	Gaussian	70.9	~350	168.72	70.0	~430	133.88
	Linear	44.7	~44000	39.198	44.7	~28000	50.451
	Cubic	81.6	~1000	253.64	81.5	~890	226.15
	Quadratic	54.6	~950	203.48	52.5	~860	215.19
160	Gaussian	68.2	~350	166.21	71.3	~460	141.00
	Linear	44.7	~55000	36.114	44.7	~58000	41.657
	Cubic	82.5	~870	259.73	81.7	~1100	228.88
	Quadratic	54.0	~640	201.86	52.5	~850	207.1
180	Gaussian	69.8	~340	151.53	71.4	~540	129.98
	Linear	44.7	~170000	31.305	44.7	~50000	34.891
	Cubic	81.6	~730	251.82	82.8	~850	221.59
	Quadratic	54.2	~700	194.44	52.6	~920	211.2
200	Gaussian	69.5	~360	199.97	69.8	~600	153.8
	Linear	44.7	~24000	63.454	44.7	~35000	66.639
	Cubic	83.6	~700	322.38	83.7	~1600	233.26
	Quadratic	53.8	~480	248.18	52.6	~1300	217.65

Table 2 summarises the performance of the hybrid modified Otsu with mathematical morphology. As in Table 1, each disk radius was evaluated using gaussian, linear, quadratic, and cubic SVM kernels both with and without PCA. The results show substantial differences among the four kernels. Without PCA, the highest classification accuracy was 84.5%, obtained using the cubic kernel at a disk radius of 80. At the same radius, applying PCA produced an accuracy of 82.5%. The cubic kernel also produced relatively high accuracies at several other radii, including 82.6% at radius 60, 82.5% at radius 160, and 83.6% at radius 200 without PCA. With PCA, the highest accuracy reported in Table 2 was 83.7% at radius 200 using the cubic kernel. At this radius, the corresponding prediction speed was approximately 1600 obs/sec, with a training time of 233.26 seconds. The results again indicate that changes in the disk radius did not lead to a uniform increase or decrease in classification performance. Instead, classification accuracy depended on the combination of segmentation configuration, SVM kernel, disk radius, and PCA setting.

Based on Tables 1 and 2, the cubic kernel provided the highest overall classification performance for both the hybrid original Otsu and hybrid modified Otsu approaches. Following the training stage, the selected configurations were evaluated using the remaining 30% of the data. The testing performance of both approaches is presented in Table 3.

Table 3

Accuracy Performance from Testing Data

Method	Radius	With PCA			Without PCA		
		%	Prediction Speed (obs/sec)	Training Time (sec)	%	Prediction Speed (obs/sec)	Training Time (sec)
Hybrid original Otsu with mathematical morphology	200	87.1	~5000	26.452	88.9	~3100	31.703
Hybrid modified Otsu with mathematical morphology	80	85.2	~4800	37.1	87.1	~1300	47.777

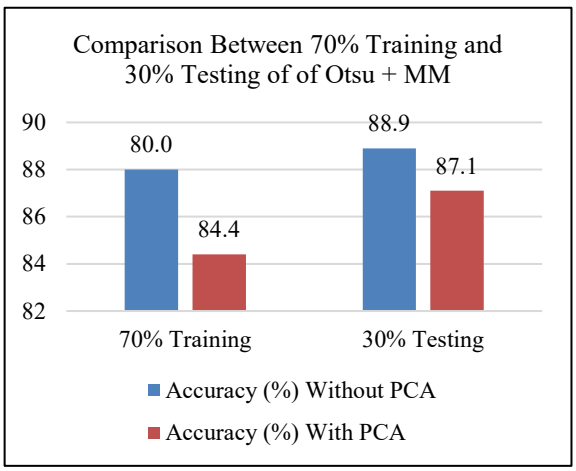
Table 3 presents the testing performance of the selected configurations, where the radius used for each method was determined based on the corresponding training results. For the hybrid original Otsu with mathematical morphology, radius 200 was selected, whereas radius 80 was used for the hybrid modified Otsu approach. The comparison considers classification accuracy, and prediction speed with and without PCA displayed in Figure 4.

Overall Performance Comparison

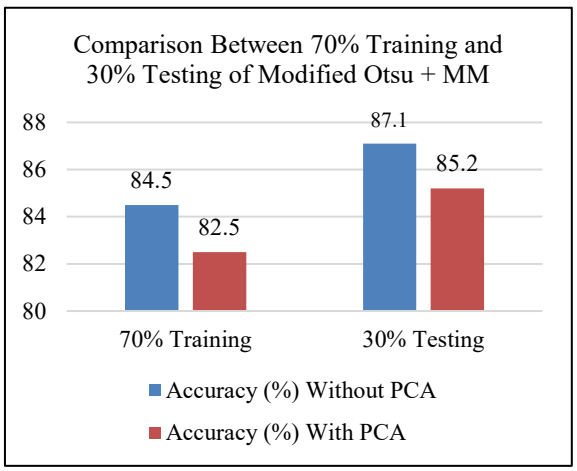
Figure 4 presents the overall performance comparison between the hybrid original Otsu and modified Otsu with mathematical morphology. The comparison includes the classification accuracy obtained from the 70% training and 30% testing datasets, and the corresponding prediction speeds with and without PCA.

Figure 4

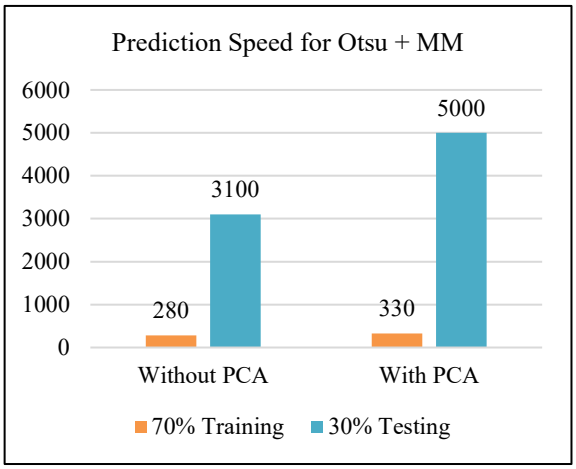
Overall Comparison for Hybrid Otsu and Modified Otsu with Mathematical Morphology



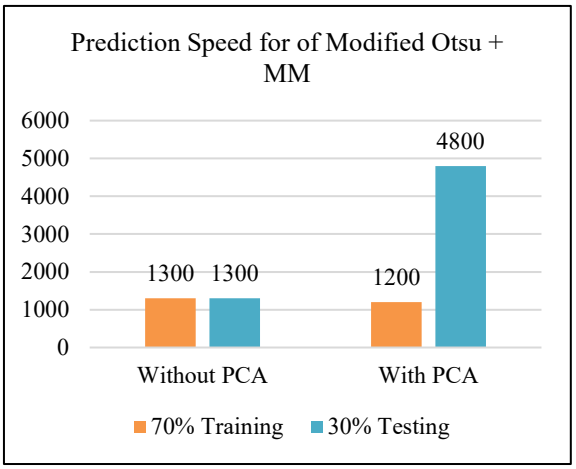
(i)



(ii)



(iii)



(iv)

Figure 4(i) compares the classification accuracy of the hybrid original Otsu with mathematical morphology at radius 200. For the 70% training dataset, the reported accuracies were 80.0% without PCA and 84.4% with PCA. When evaluated using the 30% testing dataset, the accuracies increased to 88.9% without PCA and 87.1% with PCA. Similarly, Figure 4(ii) shows that the hybrid modified Otsu with mathematical morphology at radius 80 achieved training accuracies of 84.5% without PCA and 82.5% with PCA, whereas the corresponding testing accuracies were 87.1% and 85.2%, respectively. Based on these results, the hybrid original Otsu with mathematical morphology achieved the highest reported testing accuracy of 88.9% without PCA. The computational performance of both approaches is presented in Figure 4(iii) and Figure 4(iv). For the hybrid original Otsu with mathematical morphology at radius 200, the prediction speed increased from approximately 280 obs/sec for the 70% training data to 3100 obs/sec for the 30% testing data without PCA. With PCA, the corresponding prediction speeds were approximately 330 obs/sec and 5000 obs/sec, respectively. For the hybrid modified Otsu with mathematical morphology at radius 80, the prediction speeds were approximately 1300 obs/sec for both the 70% training and 30% testing datasets without PCA, while the values obtained with PCA were approximately 1200 obs/sec and 4800 obs/sec, respectively. Overall, the results indicate that the classification performance was influenced by the segmentation approach, disk structuring-element radius, SVM kernel, and PCA setting. The hybrid original Otsu with mathematical morphology without PCA produced the highest testing accuracy among the evaluated configurations, while the cubic kernel showed the strongest overall classification performance for both segmentation approaches.

CONCLUSION

This study compared hybrid original Otsu with mathematical morphology and hybrid modified Otsu with mathematical morphology for classifying fatty, glandular, and dense breast tissue. The results showed that the hybrid original Otsu method achieved the highest testing accuracy, with 88.9% without PCA and 87.1% with PCA, compared with 87.1% and 85.2% for the modified Otsu method. This study demonstrates that disk-structuring-element radius is an important experimental parameter in a hybrid Otsu-morphology pipeline for multiclass mammographic tissue classification. Overall, the hybrid original Otsu with mathematical morphology provided better classification performance for the selected dataset and experimental settings. Future work may investigate other structuring-element shapes, radii, and classifiers to further improve classification accuracy and computational efficiency.

ACKNOWLEDGEMENT

The authors would like to acknowledge Universiti Teknologi MARA (UiTM) and Faculty of Mathematical and Computer Sciences (FSKM) for their support and contributions.

Conflict of Interest
The authors have no conflicts of interest to declare.

Non-funded
This research received no specific grant from any funding agency in the public, commercial, or not-for-profit sectors.

REFERENCES

Azman, N. F., Jumaat, A. K., Badarul Azam, A. S., Mohd Ghani, N. A. S., Maasar, M. A., Laham, M. F., & Nek Abd Rahman, N. (2024). Digital medical images segmentation by active contour model based on the signed pressure force function. *Journal of Information and Communication Technology*, *23*(3), 393–419. https://doi.org/10.32890/jict2024.23.3.2

Chunlei, L., Hao, S., Hu, W., & Yi, H. (2019). A Hybrid Algorithm of Otsu and Adaptive Region for Image Segmentation. *2019 IEEE International Conference on Power, Intelligent Computing and Systems, ICPICS 2019*, 107–110. https://doi.org/10.1109/ICPICS47731.2019.8942500

Dallali, A., El Khediri, S., Slimen, A., & Kachouri, A. (2018). Breast tumors segmentation using Otsu method and K-means. *2018 4th International Conference on Advanced Technologies for Signal and Image Processing, ATSIP 2018*, 1–6. https://doi.org/10.1109/ATSIP.2018.8364469

Gudinas, A., Moscatello, J., & Hollen, S. M. (2020). Defect identification and statistics toolbox: automated defect analysis for scanning probe microscopy images. *Journal of Physics Condensed Matter*, *33*(4). https://doi.org/10.1088/1361-648X/abc1b2

Khairnar, S., Thepade, S. D., & Gite, S. (2021). Effect of image binarization thresholds on breast cancer identification in mammography images using OTSU, Niblack, Burnsen, Thepade's SBTC. *Intelligent Systems with Applications*, *10–11*, 200046. https://doi.org/10.1016/j.iswa.2021.200046

Kumar, A., & Tiwari, A. (2019). A Comparative Study of Otsu Thresholding and K-means Algorithm of Image Segmentation. *International Journal of Engineering and Technical Research (IJETR)*, *9*(5), 12–14. https://doi.org/10.31873/ijetr.9.5.2019.62

Leutenegger, S., Chli, M., & Siegwart, R. Y. (2011). *BRISK : Binary Robust Invariant Scalable Keypoints*. 2548–2555.

Liu, L., Zhao, D., Yu, F., Heidari, A. A., Ru, J., Chen, H., Mafarja, M., Turabieh, H., & Pan, Z. (2021). Performance optimization of differential evolution with slime mould algorithm for multilevel breast cancer image segmentation. *Computers in Biology and Medicine*, *138*(October). https://doi.org/10.1016/j.compbiomed.2021.104910

Mohamad, F. S., Alsuhimat, F. M., Mohamed, M. A., Mohamad, M., & Jamal, A. A. (2018). Detection and feature extraction for images signatures. *International Journal of Engineering and Technology(UAE)*, *7*(3.28 Special Issue 28), 44–48. https://doi.org/10.14419/ijet.v7i3.28.20963

Nishiyama, K., Taira, N., Mizoo, T., Kochi, M., Ikeda, H., Iwamoto, T., Shien, T., Doihara, H., Ishihara, S., Kawai, H., Kawasaki, K., Ishibe, Y., Ogasawara, Y., & Toyooka, S. (2020). Influence of breast density on breast cancer risk: a case control study in Japanese women. *Breast Cancer*, *27*(2), 277–283. https://doi.org/10.1007/s12282-019-01018-6

Noor, N. M., Zainal, N. F., & Yasiran, S. S. (2025). Comparison of Structuring Elements for Benign and Malignant Classification in Breast Cancer. *Environment-Behaviour Proceedings Journal*, *10*(SI40), 55-63.

Palani, U., Vasanthi, D., & Rabiya Begam, S. (2020). Enhancement of Medical Image Fusion Using Image Processing. *Journal of Innovative Image Processing*, *2*(4), 165–174. https://doi.org/10.36548/jiip.2020.4.001

Remeseiro, B., & Bolon-Canedo, V. (2019). A review of feature selection methods in medical applications. *Computers in Biology and Medicine*, *112*(February), 103375. https://doi.org/10.1016/j.compbiomed.2019.103375

Singh, S., & Kumar, R. (2020). Histopathological image analysis for breast cancer detection using cubic SVM. *2020 7th International Conference on Signal Processing and Integrated Networks, SPIN 2020*, 498–503. https://doi.org/10.1109/SPIN48934.2020.9071218

Yasiran, S. S., Salleh, S., & Mahmud, R. (2020). Standard Deviation Based Otsu for Breast Cancer Classification. *ASM Science Journal*, *26*, 1–4. https://doi.org/10.32802/asmscj.2020.sm26(4.19)

This is an open access article under the CC BY-SA license (https://creativecommons.org/licenses/by-sa/4.0/).